Attenuation of Ground-Motion Amplitudes from Small-Magnitude Earthquakes in the Montney Play, Northeastern British Columbia

A. Babaie Mahani, Geoscience BC, Vancouver, BC, ali.mahani@mahangeo.com

H. Kao, Natural Resources Canada, Geological Survey of Canada-Pacific, Sidney, BC

Babaie Mahani, A. and Kao, H. (2018): Attenuation of ground-motion amplitudes from small-magnitude earthquakes in the Montney play, northeastern British Columbia; *in* Geoscience BC Summary of Activities 2017: Energy, Geoscience BC, Report 2018-4, p. 15–22.

Introduction

Analysis of local ground-motion data recorded by seismographic stations is essential in understanding the potential seismic hazard in a region. Ground-motion prediction equations (GMPE) are key elements in every seismic hazard assessment, especially at distances close to the source of shallow induced earthquakes, which have the potential of causing damage to structures close to injection sites (Novakovic and Atkinson, 2015). Near-source evaluation of ground-motion amplitudes is now possible in areas such as western Alberta and northeastern British Columbia (BC) with the recent increase in seismograph stations for the purpose of monitoring the induced seismicity from hydraulic fracturing and wastewater injection (Schultz et al., 2015; Babaie Mahani et al., 2016). The aim of this project is to analyze a rich database of ground-motion amplitudes from small-magnitude, potentially induced earthquakes in the Montney play of northeastern BC recorded at short hypocentral distance. The majority of data used in this study are from waveforms recorded by the private seismograph stations near hydraulic fracturing and wastewater injection operations. Of particular interest is understanding the characteristics of the observed ground-motion amplitudes from events with amplitudes large enough for the onset of damage. This paper details the datasets used in this study, followed by the analysis of attenuation of ground-motion amplitudes in the Montney play. Understanding the local ground-motion parameters in the study area is important for the assessment of the potential seismic hazard from induced events to infrastructure, such as the BC Hydro Site C dam on the Peace River near Fort St. John.

Database

Waveforms from local and regional broadband seismographic stations in the study area were used to analyze ground-motion amplitudes from small induced earthquakes. Most of the waveforms are from two networks of five stations operated by Canadian Natural Resources Limited (CNRL) in the Graham and Septimus areas (Figure 1) to monitor the disposal of wastewater. Waveforms from three other private networks were also used: ARC Resources Ltd. (ARC) and Encana Corporation (Encana) for monitoring of hydraulic fracturing and Canbriam Energy Inc. (Canbriam) for monitoring of hydraulic fracturing and wastewater disposal.

Besides the data from private seismograph stations, waveforms from three Canadian National Seismograph Network (CNSN) stations in the region were also included to complement the database used in this study (Figure 1). Station number 1, in the Graham area, was originally a CNRL station but converted to a CNSN station in 2016.

Waveforms from 219 local events were used in this study, of which 129 events are in the Graham area and 90 events are in the Septimus area. For the Graham area, the CNRL network recorded 123 events for the period between March 21, 2014 and August 28, 2015 while the Canbriam network recorded two events on May 1 and June 11, 2016. There are also data from four events at CNSN station 1 on December 30, 2016, April 19 and 21, 2017 and June 8, 2017. For the Septimus area, the CNRL network recorded 81 events for the period between April 16 and October 12, 2014. The ARC network recorded four events on January 14 and 16, 2017 and June 10, 2017 while the Encana seismograph station recorded five events for the period between July 15 and 29, 2017. Data from ARC also includes the waveforms from the two CNSN stations in the Septimus area (Figure 1).

A database of ground-motion amplitudes was compiled after correcting each waveform for instrument response and filtering with a high-pass, second-order Butterworth filter at a corner frequency of 0.1 hertz (Hz). Ground-motion amplitudes for peak ground acceleration (PGA), peak ground velocity (PGV) and response spectral acceleration (PSA) at frequencies of 1, 2, 3.3, 5 and 10 Hz were compiled for the vertical component and the geometric mean of the horizontal components. The available dataset contains ground-motion amplitudes from events with local magnitude (M_L) from 1.5 to 3.8 and hypocentral distance between 1.6 and 42 km (M_L 1.5–3.8 and distance between 2.3 and 19 km in

This publication is also available, free of charge, as colour digital files in Adobe Acrobat® PDF format from the Geoscience BC website: http://www.geosciencebc.com/s/SummaryofActivities.asp.

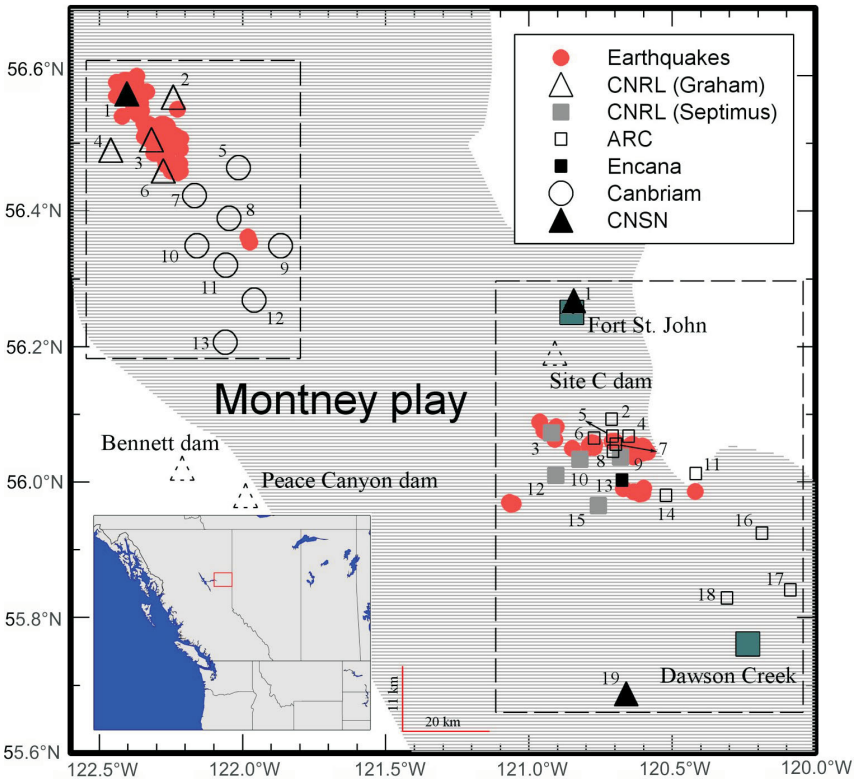

Figure 1. Map of part of the Montney play of northeastern British Columbia and distribution of the earthquakes and stations used in this study. Boxes show the Graham (northwest) and Septimus (southeast) areas with stations numbered in each area. Triangles with stations numbered in each area. Triangles with dashed outlines mark the approximate locations of BC Hydro dams. The inset shows the location of the study area in British Columbia. Abbreviations: ARC, ARC Resources Ltd.; Canbriam, Canbriam Energy Inc.; CNRL, Canadian Natural Resources Limited; CNSN, Canadian National Seismograph Network; Encana, Encana Corporation.

the Graham area and M_L 1.5–3.0 and distance between 1.6 and 42 km in the Septimus area). Most of the ground-motion amplitudes used in this study are from events with magnitude <2 and focal depth between 3 and 4 km. No event in this dataset is deeper than 8 km (for events with unknown depths, a value of 2 km was assigned).

Due to the shallow depth of induced events, damage can still be expected from small earthquakes at short hypocentral distance. Worden et al. (2012) analyzed the relationship between ground-motion amplitudes (PGA and PGV) versus modified Mercalli intensity (MMI) in California. Based on their results, the onset of damage (MMI at level VI; Wald et al., 1999) corresponds to PGA between 50 and 300 cm/s^2 and PGV between 3.8 and 24 cm/s. For the dataset used in this study, all PGA values are below the lower bound for the onset of damage (<50 cm/s^2). At the hypocentral distance of ~2.6 km, however, a relatively large ground acceleration was recorded at one of the ARC seismographic stations (station 8, Figure 1) with a maximum PGA value of ~115 cm/s^2 on the east-west component from an M_L 3 event. In Figure 2, the three-component waveforms from the three events recorded at stations 8 and 5 (closer to the source) are shown. Since events are very close in space, the hypocentral distance to station 5 is ~2.2 km whereas it is ~2.6 km for station 8. It is clear in Figure 2 that PGA is higher at station 8 for all three events and components despite the larger hypocentral distance. Local site condition or radiation pattern might be the reason for the larger observed ground motion at this station.

Attenuation of Ground-Motion Amplitudes

One of the key parameters in seismic hazard assessment is the GMPE, which describes the amplitudes of motions and their attenuation for given magnitude, distance and site condition. Understanding the expected level of ground motion from local seismic events at infrastructure such as the BC Hydro Site C dam (Figure 1) helps with the mitigation of seismic hazard from events caused by fluid injection. This information can also be used for implementation of exclusion zones around critical infrastructures. For this study area, a GMPE has been developed for the geometric mean of the horizontal components of motion, using the ground-motion amplitudes described in the 'Database' section above. These amplitudes have been corrected to the reference site condition with an average shear-wave velocity in the top 30 m (Vs_{30}) of 760 m/s, using the linear component of correction factors provided by Boore et al. (2014) and the estimated Vs_{30} values of Babaie Mahani and Kao (in press) for each seismograph station in the study area. For the purpose of this study, the datasets from the Graham and Septimus areas have been combined. In order to understand the differences in ground motion between the two areas, the ratio of ground-motion amplitudes (Graham to Septimus) were calculated for magnitude and distance bins using the geometric mean of the horizontal components of motion corrected to the reference site condition (Vs_{30} = 760 m/s) in each region. Overall, ground motions are comparable between the two areas with the exception of some frequencies at magnitude bin 2.5–3.0.

The Atkinson (2015) ground-motion model was used for the development of local GMPE as

$$\log Y = c_0 + c_1 M + c_2 M^2 + c_3 \log R \qquad 1$$

where Y is the observed geometric mean of the horizontal components of ground-motion amplitude (e.g., PGA) corrected to the reference site condition (Vs_{30} = 760 m/s). M is

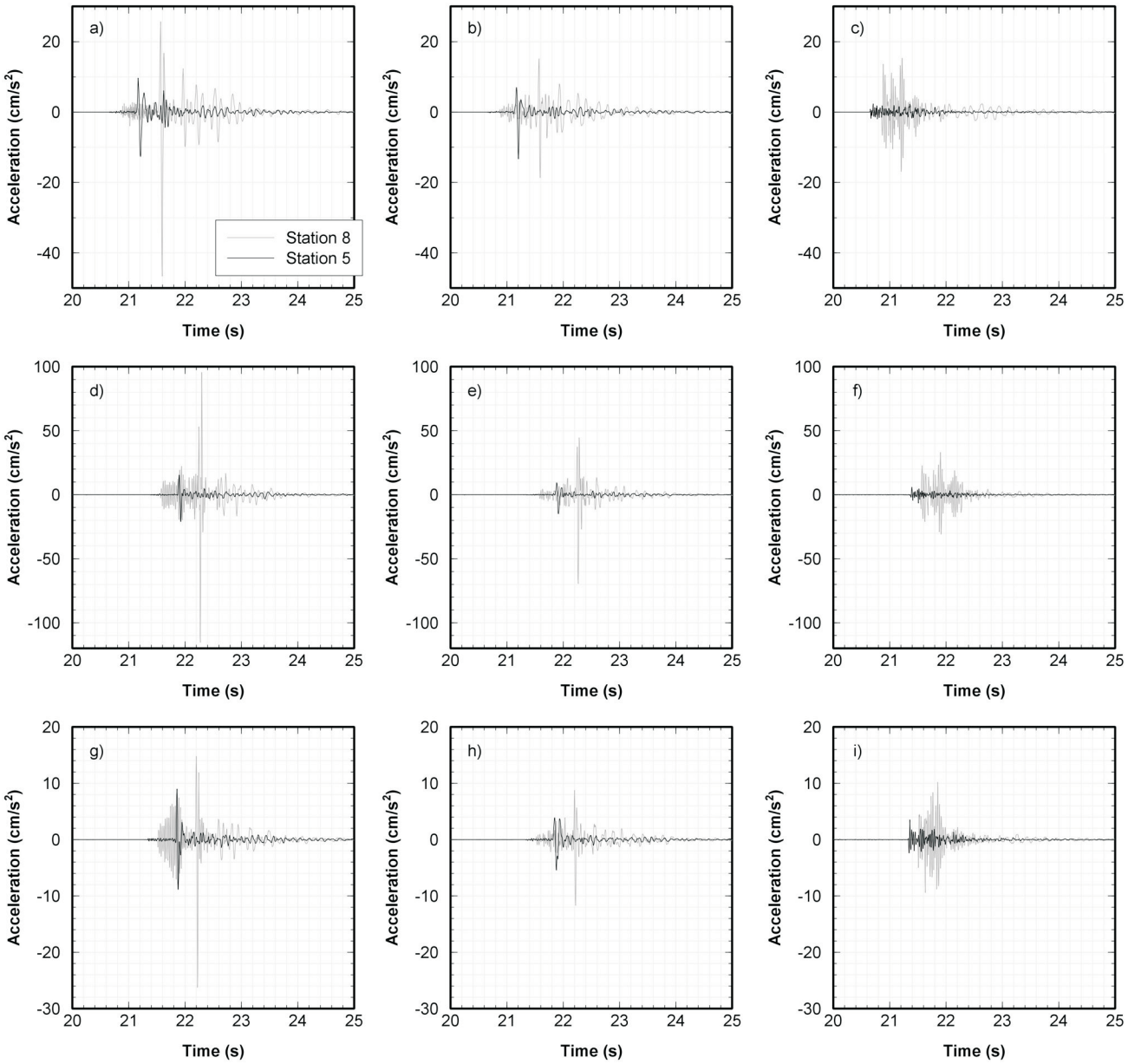

Figure 2. Waveforms of the three events recorded by stations 5 and 8 of the ARC Resources Ltd. seismograph network (northeastern British Columbia; Figure 1). Panels **a)**, **d)** and **g)** are the east-west component, **b)**, **e)** and **h)** are the north-south component, and **c)**, **f)** and **i)** are the vertical component. Top and middle rows are from events with local magnitude 3 and the bottom row is from an event with local magnitude 2.5.

magnitude and R is the effective distance that includes near-source distance-saturation effects using an effective depth parameter, h,

$$R = \sqrt{R_{hypo}^2 + h^2} \qquad 2$$

In equation (2), R_{hypo} is hypocentral distance and h is set as

$$h = \max(1, 10^{(-1.72 + 0.43M)}) \qquad 3$$

The parameters of equation (1) were determined in two steps. In the first step, the distance dependence is determined through calculation of the geometrical spreading coefficient (c_3) along with a source term for each earthquake. In the second step, the magnitude dependency is analyzed by obtaining the coefficients c_0, c_1 and c_2 through the regression between the source terms and event magnitudes using the first three terms in equation (1). Table 1 presents these coefficients determined for the combined dataset used in this study. In Table 1, σ_{intra} and σ_{inter} are the intra-event and inter-event components of standard deviation of the residuals (difference, in log unit, between the observed and predicted values). The total standard deviation was obtained as

$$\sigma_{total} = \sqrt{\sigma_{intra}^2 + \sigma_{inter}^2} \qquad 4$$

Table 1. Coefficients of the regression model (equation 1) for the geometric mean of the horizontal components (corrected for reference site condition with an average shear-wave velocity in the top 30 m [Vs_{30}] of 760 m/s) of peak ground acceleration (PGA), peak ground velocity (PGV) and response spectra acceleration (PSA) at frequencies 1, 2, 3.3, 5 and 10 hertz (Hz) using the combined dataset from the Graham and Septimus areas, northeastern British Columbia.

	c_0	c_1	c_2	c_3	σ_{intra}	σ_{inter}	σ_{total}
PGA	–0.11	0.52	0.07	–2.35	0.33	0.19	0.38
PGV	–2.08	0.55	0.08	–2.29	0.32	0.17	0.36
PSA 10 Hz	–0.11	0.71	0.03	–2.15	0.32	0.17	0.36
PSA 5 Hz	–0.75	0.85	0.02	–2.11	0.31	0.16	0.35
PSA 3.3 Hz	–1.18	0.79	0.04	–1.98	0.26	0.14	0.29
PSA 2 Hz	–1.59	0.73	0.06	–2.07	0.23	0.16	0.29
PSA 1 Hz	–2.49	0.77	0.06	–1.98	0.23	0.16	0.28

Figure 3 shows the residuals from equation (1) for PGA and PGV versus hypocentral distance and magnitude. Overall, there are no trends in the residuals and their mean values are close to zero for the distance and magnitude ranges considered in this study when sufficient number of data are available (hypocentral distance 3–20 km and magnitude 1.5–3.5).

Figure 4 shows the attenuation models for different magnitudes along with the observed ground-motion amplitudes

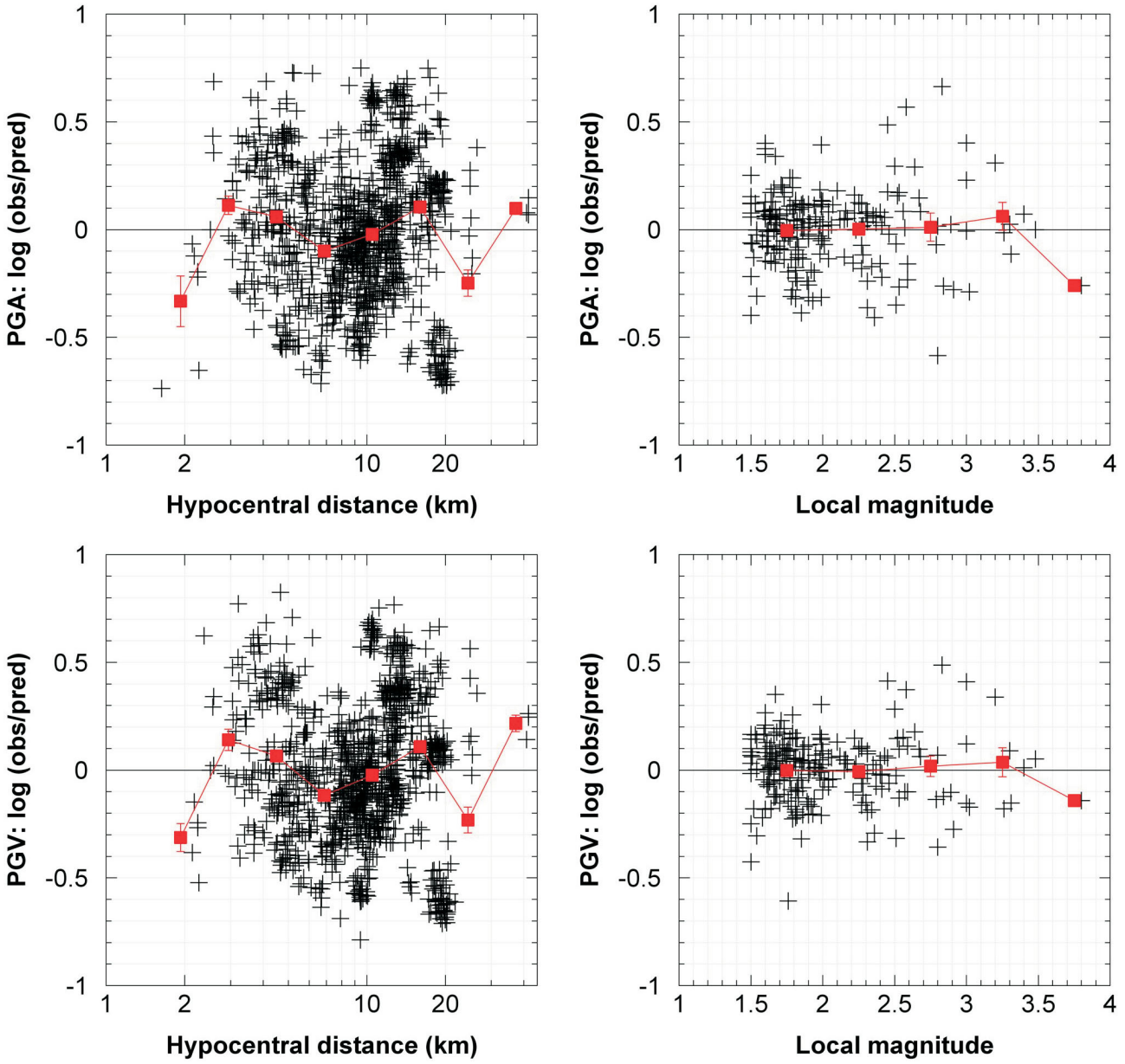

Figure 3. Residuals, defined as the difference (in log unit) between the observed (obs) and predicted (pred) values of peak ground acceleration (PGA) and peak ground velocity (PGV) from equation (1), versus hypocentral distance and local magnitude (Graham and Septimus areas, northeastern British Columbia). Squares are the mean values of residuals determined for logarithmically spaced distance and equally spaced magnitude bins and the error bars are the standard error about the mean.

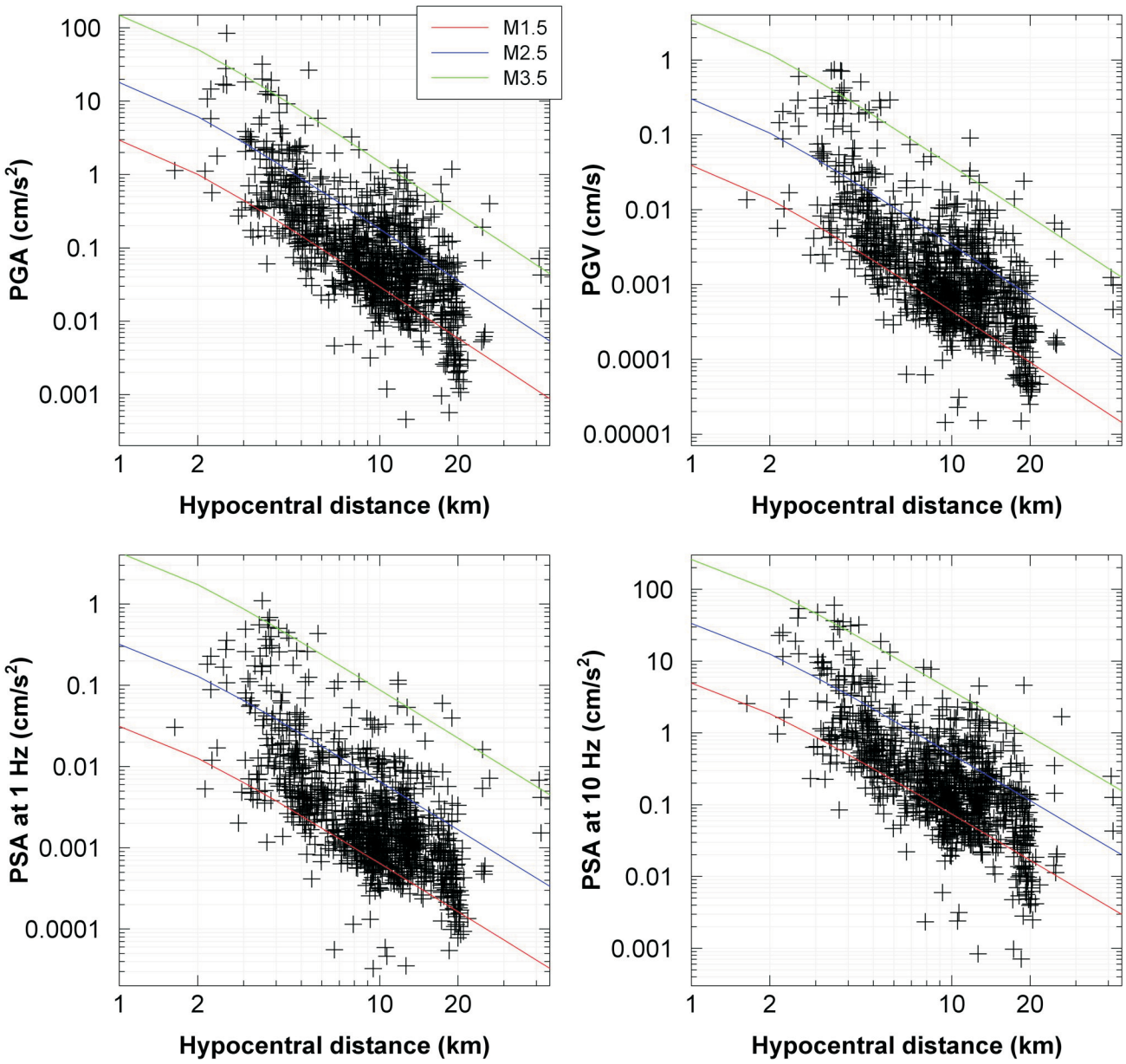

Figure 4. Geometric mean of the horizontal components of motion, corrected for the reference site condition (average shear-wave velocity in the top 30 m [Vs_{30}] of 760 m/s), for peak ground acceleration (PGA), peak ground velocity (PGV) and response spectral acceleration (PSA) at frequencies 1 and 10 hertz (Hz). Also plotted are the prediction models for different magnitudes (red, blue, green lines) using equation (1) and Table 1.

(geometric mean of the horizontal components corrected to the reference site condition) for PGA, PGV and PSA at frequencies 1 and 10 Hz. Geometrical spreading coefficients obtained for ground-motion amplitudes in this study's combined dataset suggest a higher decay rate in the amplitudes with distance than those obtained in Atkinson (2015) using the Next Generation Attenuation-West 2 database (Bozorgnia et al., 2014) for short hypocentral distance (<40 km). For example, in Atkinson (2015), the geometrical spreading coefficient of –1.75 was calculated for the attenuation of PGA whereas a value of –2.35 was obtained in this study (Table 1). The difference in the geometrical spreading attenuation between this study and Atkinson (2015) is most likely due to the different magnitude range considered in the two studies. Whereas the database in Atkinson (2015) includes earthquakes with magnitude 3–6, this study's database only contains smaller earthquakes with magnitude 1.5–3.8. This is an important observation to consider if ground-motion amplitudes from larger magnitude events (e.g., >4) are to be estimated in the Montney play area using the GMPE developed in this study (i.e., this model will likely underestimate ground motions for events with magnitudes >4).

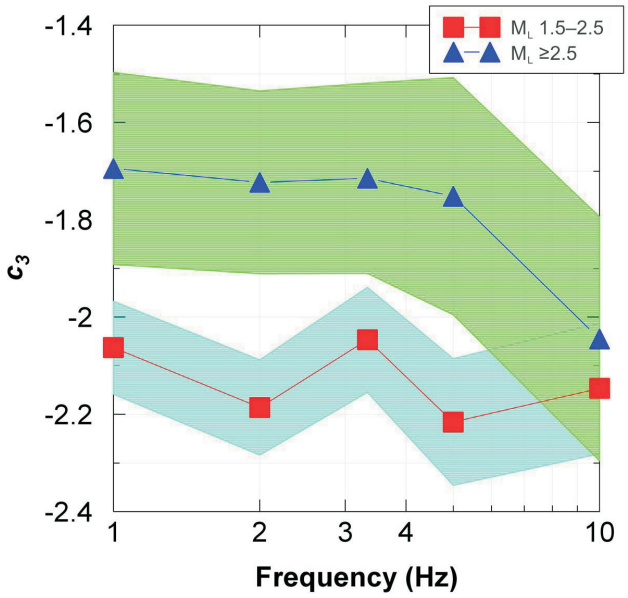

Figure 5. Coefficient of geometrical spreading attenuation (c_3 in equation 1) versus frequency (hertz [HZ]) for two local magnitude (M_L) bins, M_L 1.5–2.5 and M_L ≥2.5 (Montney play, northeastern British Columbia). Shaded regions show the 95% confidence intervals in the estimation of c_3.

To further analyze the change in the geometrical spreading attenuation of ground-motion amplitudes, its coefficient (c_3) was calculated, using equation (1), for two magnitude bins, M_L 1.5–2.5 and M_L ≥2.5, and the results are shown in Figure 5. It is clear that the ground-motion amplitudes from the lower magnitude bin (M_L 1.5–2.5) attenuate faster than those with larger magnitudes (M_L ≥2.5). The difference between the geometrical spreading attenuation becomes minimal at higher frequencies (10 Hz). This is also true for PGV and PGA (not shown).

Conclusions

Attenuation of peak ground acceleration (PGA), peak ground velocity (PGV) and response spectral acceleration (PSA) at frequencies 1, 2, 3.3, 5 and 10 Hz from potentially induced events in the Montney play of northeastern British Columbia were analyzed for this project. The dataset used included waveforms from 219 events with local magnitude (M_L) ranging from 1.5 to 3.8 recorded at hypocentral distance of <45 km. Waveforms were supplied by local seismographic stations operated by energy companies and complemented with some waveforms from the regional seismographic stations of the Canadian National Seismograph Network. The Atkinson (2015) ground-motion prediction equation (GMPE) was used and its coefficients for ground-motion amplitudes were obtained for the Montney play area. Analysis of the geometrical spreading attenuation of ground-motion amplitudes from events with magnitude ranges of M_L 1.5–2.5 and M_L ≥2.5 suggests a lower decay rate for the larger magnitude events, especially for frequencies <10 Hz. This is an important observation to consider if ground-motion amplitudes from larger magnitude events (e.g., magnitudes >4) are to be estimated in the Montney play area using the GMPE developed in this study (i.e., this model will likely underestimate ground motions for events with magnitudes >4).

Acknowledgments

This investigation would not be possible without contributions from the local oil and gas operators. The authors would like to thank N. Orr and A. Gamp from Canadian Natural Resources Limited for sharing the waveforms of more than 200 earthquakes recorded by their seismograph networks in the Graham and Septimus areas. Canbriam Energy Inc., ARC Resources Ltd. and Encana Corporation also contributed waveforms to this study. S. Venables from BC Oil and Gas Commission is especially thanked for his effort in the acquisition of waveform data. This project was supported by the BC Seismic Research Consortium (BC Oil and Gas Commission, Geoscience BC, BC Oil and Gas Research and Innovation Society, Canadian Association of Petroleum Producers and Yukon Geological Survey).

Natural Resources Canada, Lands and Minerals contribution 20170243

References

Atkinson, G.M. (2015): Ground-motion prediction equation for small-to-moderate events at short hypocentral distances, with application to induced-seismicity hazards; Bulletin of Seismological Society of America, v. 105, p. 981–992, URL <https://pubs.geoscienceworld.org/bssa/article-abstract/105/2A/981/332710/> [November 2017].

Babaie Mahani, A. and Kao, H. (in press): Ground motion from M1.5-3.8 induced earthquakes at hypocentral distance <45 km in the Montney play of northeast British Columbia, Canada; Seismological Research Letters.

Babaie Mahani, A., Kao, H., Walker, D., Johnson, J. and Salas, C. (2016): Performance evaluation of the regional seismograph network in northeast British Columbia, Canada, for monitoring of induced seismicity; Seismological Research Letters, v. 87, p. 648–660, URL <http://srl.geoscienceworld.org/content/87/3/648> [November 2017].

Boore, D.M., Stewart, J.P., Seyhan, E. and Atkinson, G.M. (2014): NGA-West2 equations for predicting PGA, PGV, and 5% damped PSA for shallow crustal earthquakes; Earthquake Spectra, v. 30, p. 1057–1085, URL <http://earthquakespectra.org/doi/10.1193/070113EQS184M> [November 2017].

Bozorgnia, Y., Abrahamson, N.A., Al Atik, L., Ancheta, T.D., Atkinson, G.M., Baker, J.W., Baltay, A., Boore, D.M., Campbell, K.W., Chiou, B.S.-J., Darragh, R., Day, S., Donahue, J., Graves, R.W., Gregor, N., Hanks, T., Idriss, I.M., Kamai, R., Kishida, T., Kottke, A., Mahin, S.A., Rezaeian, S., Rowshandel, B., Seyhan, E., Shahi, S., Shantz, T., Silva, W., Spudich, P., Stewart, J.P., Watson-Lamprey, J., Wooddell, K. and Youngs, R. (2014): NGA-West2 research project; Earthquake Spectra, v. 30, p. 973–

987, URL <http://earthquakespectra.org/doi/10.1193/072113EQS209M> [November 2017].

Novakovic, M. and Atkinson, G.M. (2015): Preliminary evaluation of ground motions from earthquakes in Alberta; Seismological Research Letters, v. 86, p. 1086–1095, URL <http://srl.geoscienceworld.org/content/86/4/1086> [November 2017].

Schultz, R., Stern, V., Gu, Y.J. and Eaton, D. (2015): Detection threshold and location resolution of the Alberta Geological Survey Earthquake Catalogue; Seismological Research Letters, v. 86, p. 385–397, URL <http://srl.geoscienceworld.org/content/86/2A/385> [November 2017].

Wald, D.J., Quitoriano, V., Heaton, T.H. and Kanamori, H. (1999): Relationships between peak ground acceleration, peak ground velocity, and Modified Mercalli Intensity in California; Earthquake Spectra, v. 15, p. 557–564, URL <http://earthquakespectra.org/doi/10.1193/1.1586058> [November 2017].

Worden, C.B., Gerstenberger, M.C., Rhoades, D.A. and Wald, D.J. (2012): Probabilistic relationships between ground-motion parameters and Modified Mercalli Intensity in California; Bulletin of Seismological Society of America, v. 102, p. 204–221, URL <https://pubs.geoscienceworld.org/bssa/article-abstract/102/1/204/349630/> [November 2017].